

## Research Article

# Impact of SiO<sub>2</sub> Modification on the Performance of Nafion Composite Membrane

Shuangjie Liu,<sup>1</sup> Jialin Yu<sup>1</sup> ,<sup>1</sup> Yongping Hao,<sup>1</sup> Feng Gao,<sup>1</sup> Mo Zhou,<sup>1</sup> and Lijun Zhao<sup>2</sup>

<sup>1</sup>School of Equipment Engineering, Shenyang Ligong University, Shenyang 110168, China

<sup>2</sup>Hua'an Industry Group Co., Ltd, 161046, China

Correspondence should be addressed to Jialin Yu; 641696907@qq.com

Received 25 July 2023; Revised 28 November 2023; Accepted 19 December 2023; Published 8 January 2024

Academic Editor: Zhi Li

Copyright © 2024 Shuangjie Liu et al. This is an open access article distributed under the Creative Commons Attribution License, which permits unrestricted use, distribution, and reproduction in any medium, provided the original work is properly cited.

Using Nafion212 membrane and TEOS solution as raw materials, Nafion212/SiO<sub>2</sub> composite membranes were prepared. In the in situ sol-gel reaction process, a series of Nafion/SiO<sub>2</sub> composite membranes were prepared by varying the reaction temperature and reaction time. The effects of different modification schemes on Nafion/SiO<sub>2</sub> composite membranes were studied using SEM, EDS, TEM, TGA, XRD, and mechanical tensile experiments, among other methods. The results show that Nafion/SiO<sub>2</sub> composite membranes prepared at 3°C exhibit a well-separated phase structure and excellent water retention properties, with a water uptake of 29.23% and a swelling ratio of 24.25%. These membranes also demonstrate outstanding physical and chemical performance, with a maximum tensile stress of 13.6 MPa and an elongation at a break of 270%. At 110°C, the proton conductivity of the Nafion/SiO<sub>2</sub> composite membrane reaches 0.172 S/cm, meeting the requirements for high-temperature proton exchange membrane fuel cells.

## 1. Introduction

Since the beginning of the 21st century, environmental pollution has become increasingly severe, while the reserves of nonrenewable energy sources are diminishing. Renewable and green energy sources have attracted widespread attention. New energy primarily includes wind energy, solar energy, hydrogen energy, and other renewable energy sources. Fuel cells, as a key research focus in new energy development, have experienced rapid advancements in recent years [1]. Currently, the main fuels for fuel cells are hydrogen, methanol, and natural gas, which are renewable or have significant reserves. Compared to traditional hydro-power and wind power generation, fuel cells have a relatively simple structure, smaller size, and broader range of applications, with promising prospects in both military and civilian sectors. Hydrogen fuel cells, as a new green energy source, utilize hydrogen and oxygen as fuels and convert the chemical energy in the fuel into electrical energy through catalysts, producing only pure water as the byproduct. This reaction process complies with China's carbon emission standards

and is an important strategic goal for future energy development in our country [2]. Among hydrogen fuel cells, proton exchange membrane fuel cells (PEMFCs) have advantages such as high voltage, high energy density, and ease of operation, making them a key research direction in hydrogen fuel cell technology [3]. The operating temperature of PEMFCs typically ranges from 60°C to 80°C. Increasing the operating temperature of fuel cells can accelerate the electrode's kinetic reaction rate, address the issue of carbon monoxide poisoning, and reduce the difficulty in water-thermal management design, thereby expanding the range of fuel cell applications [4, 5]. To raise the operating temperature of PEMFCs, research and optimization of catalysts and proton exchange membranes are necessary.

The proton exchange membrane (PEM) is one of the core components of proton exchange membrane fuel cells (PEMFCs). It is located in the middle of the fuel cell, separating the anode and cathode. During the operation of the fuel cell, the proton exchange membrane provides a pathway for proton transport. Therefore, the proton exchange membrane requires a material with polymer separation

characteristics. Perfluorosulfonic acid ionomers, such as Nafion, are widely used in the field of electrochemistry due to their excellent proton permeability, chemical stability, and structural stability. Nafion, produced by DuPont in the United States, is the most mature and widely used proton exchange membrane [6]. Nafion membranes exhibit high proton conductivity, mechanical strength, and chemical stability at temperatures ranging from 60°C to 80°C.

Through specific applications in fuel cells, limitations in the performance of Nafion membranes have been observed. Research has indicated that Nafion membranes exhibit a significant decrease in performance under conditions of low humidity and high temperature. Therefore, it is necessary to consider humidity control in fuel cell design. Additionally, the high cost of Nafion membranes limits their application in certain areas. Jung and Kim [7] conducted a study on the thermal resistance of Nafion 117 membranes. The results showed that the glass transition temperature of Nafion 117 membranes occurs between 125°C and 132°C, and at 140°C, the Nafion 117 membrane assumes a crystalline state with a substantial reduction in proton conductivity and water absorption capacity. To enhance the performance of proton exchange membranes at high temperatures, further research and improvements are required. In addition to researching new materials for manufacturing proton exchange membranes, another effective method for high-temperature proton exchange membranes is the addition of high-temperature modified modifiers to the Nafion matrix. This is currently a key research direction for high-temperature proton exchange membranes. The current modification methods mainly involve inorganic fillers and organic blending modifications. The doping of inorganic fillers can enhance the water retention capability of Nafion membranes, thereby improving their performance in high-temperature environments. Organic blending modification refers to the process of modifying a blend of two or more organic materials with distinct molecular structures through physical mixing or solvent dissolution.

Di Noto et al. [8] studied the effects of SiO<sub>2</sub> nanoparticles on the structure, properties, and conductivity mechanism of Nafion composite membranes. Composite membranes with different SiO<sub>2</sub> contents were prepared using a solvent casting method, and the thermal stability of the composite membrane was found to reach 170°C through thermogravimetric testing. Ke et al. [9] prepared Nafion/SiO<sub>2</sub> composite membranes using an in situ sol-gel method. By adjusting the solvent dosage, Nafion/SiO<sub>2</sub> composite membranes with different diameters of SiO<sub>2</sub> nanoparticles were obtained. Experimental results showed that the composite membrane exhibited favorable physical and chemical properties when the diameter of SiO<sub>2</sub> nanoparticles was 10 nm. Single-cell tests were conducted at a working temperature of 110°C, and the cell using Nafion/SiO<sub>2</sub> (10 nm) showed an output voltage of 0.625 V at 600 mA/cm<sup>2</sup>, which was 50 mV higher than that of the unmodified Nafion membrane. Lin et al. [10] improved the proton conductivity of the membrane by grafting organic sulfonic acid (-SO<sub>3</sub>H) onto the surface of mesoporous silica, resulting in a significant enhancement compared to the original SiO<sub>2</sub> fillers.

According to test results, the doped organic sulfonic acid (-SO<sub>3</sub>H) fillers exhibited a more uniform distribution. Zhao et al. [11], based on organic sulfonic acid, added MnO<sub>2</sub> as a modifier to reduce the corrosion of the membrane by hydrogen peroxide. When filling the membrane with SiO<sub>2</sub>, the filler undergoes hydrolysis during the reaction, producing a large number of ethanol molecules, directly leading to a decrease in the mechanical strength of the proton exchange membrane [12]. Choi et al. [13] introduced a multifunctional dendritic Nafion/CeO<sub>2</sub> structure into the interface cathode side between the membrane and catalyst layer using electrospinning deposition. The moisture absorption effect of CeO<sub>2</sub> was utilized to enhance the water retention capacity of the composite membrane, while CeO<sub>2</sub> nanoparticles exhibited antioxidant properties at the front end of the membrane, improving the chemical durability of the fuel cell. Wang et al. [14] incorporated SiO<sub>2</sub> nanofibers doped with four functional amino acids (cysteine, serine, lysine, and glycine) into Nafion membranes using electrospinning technology. The introduction of biofunctionalized SiO<sub>2</sub> nanofibers significantly improved the proton conductivity, dimensional stability, and methanol permeability of the composite membrane. Although modification approaches for Nafion membranes have been proven to effectively enhance their performance in high-temperature environments, the synthesis processes are complex and challenging for large-scale production, making it difficult to meet practical demands. Therefore, when designing Nafion membrane modification strategies, it is important to ensure proton conductivity, chemical stability, and mechanical strength at high temperatures while considering the simplicity of the preparation method.

The present study is aimed at enhancing the fabrication efficiency of composite membranes. The in situ sol-gel method was selected for improvement to prepare Nafion212/SiO<sub>2</sub> composite membranes under low-temperature conditions. The microstructure of the Nafion212/SiO<sub>2</sub> composite membranes and the doping status of SiO<sub>2</sub> were characterized using SEM, EDS, XRD, and FT-IR experiments. TGA and mechanical analysis experiments were conducted to assess the macroscopic properties of the prepared Nafion212/SiO<sub>2</sub> composite membranes and use the two-electrode method to test the proton conductivity of the composite membrane. The effects of different doping temperatures and times on the performance of the Nafion212/SiO<sub>2</sub> composite membranes were investigated.

## 2. Materials and Methods

**2.1. Materials.** The materials used in this study were Nafion212 membranes (DuPont, USA), tetraethyl orthosilicate (TEOS, 99%, Shanghai Aladdin Biochemical Technology Co., Ltd.), methanol (chromatographic grade, Tianjin Concord Co., Ltd.), sulfuric acid (98%, Westlake Chemical Corporation), hydrogen peroxide (analytical grade, Tianjin Guangfu Fine Chemical Research Institute), deionized water.

**2.2. Composite Membrane Preparation.** Nafion212/SiO<sub>2</sub> composite membranes were prepared using tetraethyl

orthosilicate as the raw material through an in situ sol-gel reaction [9]. Tetraethyl orthosilicate (TEOS) serves as the precursor for  $\text{SiO}_2$ . The controllability of TEOS is good, allowing precise control of its concentration and processing conditions in the experiment. Its good solubility in organic solvents ensures uniform doping of silica within the membrane. The hydrolysis reaction of TEOS does not result in significant energy consumption, ensuring the proton conductivity and structural stability of the Nafion membrane. The specific procedure is as follows: Firstly, the Nafion212 membrane was dried in a vacuum oven at  $80^\circ\text{C}$  for 12 hours. Subsequently, the membrane was immersed in a  $\text{CH}_3\text{OH}/\text{H}_2\text{O}$  solution (3:2,  $30^\circ\text{C}$ ) for 1 hour. After removing the sample, the residual liquid on the membrane surface was wiped off with filter paper. Then, the sample was immersed in a  $\text{CH}_3\text{OH}/\text{TEOS}$  solution (1:2,  $30^\circ\text{C}$ ) for an in situ sol-gel reaction. The reaction was allowed to proceed for 3 minutes. After completion of the reaction, the sample was dried in a vacuum oven at  $80^\circ\text{C}$  for 48 hours, resulting in the Nafion/ $\text{SiO}_2$  composite membrane.

Following the preparation of the composite membrane, a posttreatment was performed to remove organic impurities remaining on the surface. The membrane was immersed in a 3%  $\text{H}_2\text{O}_2$  solution at  $80^\circ\text{C}$  for 1 hour. After the immersion, the composite membrane was rinsed with deionized water. Then, the membrane was immersed in 4.7%  $\text{H}_2\text{SO}_4$  at  $80^\circ\text{C}$  for protonation treatment. After completion, the composite membrane was repeatedly soaked in deionized water to remove any residual acidic substances until the pH paper indicated neutrality. Finally, the composite membrane was placed in a vacuum oven at  $80^\circ\text{C}$  for 48 hours to undergo vacuum drying.

The aforementioned procedure resulted in the preparation of a Nafion/ $\text{SiO}_2$  composite membrane. This posttreatment process effectively eliminated organic impurities and ensured the membrane was protonated and dried thoroughly.

**2.2.1. Preparation of Nafion/ $\text{SiO}_2$  Composite Membranes under Low-Temperature Conditions.** Nafion212/ $\text{SiO}_2$  composite membranes were prepared under low-temperature conditions through an in situ sol-gel reaction using tetraethyl orthosilicate (TEOS) as the raw material. The detailed procedure is as follows: firstly, the Nafion212 membrane was dried in a vacuum oven at  $80^\circ\text{C}$  for 12 hours. Then, the dried membrane was immersed in a  $\text{CH}_3\text{OH}/\text{H}_2\text{O}$  solution (3:2,  $30^\circ\text{C}$ ) for 1 hour. Subsequently, the sample was removed, and the residual liquid on the membrane surface was wiped off with filter paper. The sample was then immersed in a  $\text{CH}_3\text{OH}/\text{TEOS}$  solution (1:2,  $3^\circ\text{C}$ ) for an in situ sol-gel reaction. The reaction was carried out for 3 minutes and 5 minutes, respectively. After the reaction, the sample was kept in a vacuum oven at  $80^\circ\text{C}$  for 48 hours, resulting in the formation of Nafion/ $\text{SiO}_2$ 3°C-3 and Nafion/ $\text{SiO}_2$ 3°C-5 composite membranes. Posttreatment of the composite membranes was performed following the same procedure as described in Section 2.2.

**2.3. Characterization Method.** The doping ratio of  $\text{SiO}_2$  in the Nafion membrane modified with  $\text{SiO}_2$  was characterized

by measuring the mass of the Nafion membrane before and after  $\text{SiO}_2$  doping. The doping ratio of  $\text{SiO}_2$  in the modified Nafion membrane can be calculated using the following equation:

$$\text{Si uptake} = \frac{W_{\text{wet}} - W_{\text{dry}}}{W_{\text{dry}}} \times 100\%, \quad (1)$$

where  $W_{\text{wet}}$  represents the mass of the thin film in the wet state after  $\text{SiO}_2$  doping and  $W_{\text{dry}}$  represents the mass of the dry film before  $\text{SiO}_2$  doping.

The microstructure and distribution of silicon elements in the proton exchange membrane were characterized using a Hitachi S-4800 scanning electron microscope. The proton exchange membrane was cut into appropriate sizes and subjected to gold sputter coating on the surface. For the cross-sectional characterization of the membrane, the membrane was frozen using liquid nitrogen and then subjected to a brittle fracture treatment to ensure the integrity of the internal structure of the membrane.

Infrared spectroscopy can be used to detect the chemical composition of the tested membrane. As the wavelength changes, the molecules inside the proton exchange membrane absorb infrared light at specific wavelengths, causing vibration or rotation of the chemical bonds between the molecules. After absorption of specific wavelengths of infrared light, absorption bands appear on the spectrum. Each functional group has specific absorption bands, allowing for analysis of the functional groups in the sample using Fourier-transform infrared spectroscopy (FT-IR). In this study, the Thermo Nicolet IS5 Fourier-transform infrared spectrometer was selected for measurement, with a scanning range of  $4000\text{--}500\text{ cm}^{-1}$ .

X-ray diffraction (XRD) can be employed to examine the crystal structure of the test membrane, thereby providing information about the crystal lattice structure, lattice constants, and crystallinity of the proton exchange membrane. This allows for an understanding of the doping status of materials within the proton exchange membrane, as well as the membrane's proton conductivity properties. In this study, a D/max-rB X-ray diffractometer was selected for sample measurement. Prior to testing, the proton exchange membrane was placed in a vacuum drying oven and dried at  $80^\circ\text{C}$  for 24 hours, after which the membrane was cut into small pieces measuring  $1\text{ cm} \times 1\text{ cm}$ . The testing conditions were as follows:  $\text{CuK}\alpha$  X-ray source with a wavelength ( $\lambda$ ) of  $1.540598\text{ \AA}$ , Ni filtration. The scanning voltage, step size, and speed were set at 40 kV, 40 mA,  $2\theta = 0.01^\circ$ , and 0.05 sec/step.

Water is an important conducting medium during the proton conduction process in proton exchange membranes. In high-temperature environments, the water retention capacity and water absorption ability of the proton exchange membrane are crucial. The membrane was cut into a size of  $5\text{ cm} \times 5\text{ cm}$  and kept in a vacuum oven at  $80^\circ\text{C}$  for 24 hours to measure the dry weight of the membrane. Subsequently, the membrane was soaked in deionized water for 24 hours, removed, and quickly dried on the surface using filter paper.

The wet membrane was then weighed. The water absorption rate of the membrane is calculated using the following equation:

$$\text{WU}(\%) = \frac{W_{\text{wet}} - W_{\text{dry}}}{W_{\text{dry}}} \times 100\%. \quad (2)$$

In the equation, WU represents the water absorption rate,  $W_{\text{wet}}$  represents the weight of the wet membrane, and  $W_{\text{dry}}$  represents the weight of the dry membrane.

The length, width, and thickness of the dry and wet membranes were measured, and the volume swelling ratio was calculated using the formula shown as follows:

$$\text{SR} = \frac{(L_d \times T_d \times D_d)}{(L_w \times T_w \times D_w)} \times 100\%. \quad (3)$$

In the equation, SR represents the volume swelling ratio,  $L_d/L_w$  represents the length of the dry/wet membrane,  $T_d/T_w$  represents the width of the dry/wet membrane, and  $D_d/D_w$  represents the thickness of the dry/wet membrane.

Thermogravimetric analysis (TGA) can be employed to analyze the thermal stability of composite membranes. By controlling the temperature using a programmed procedure, the mass of the composite membrane is measured against temperature changes using a thermobalance. As the temperature increases, the composite membrane undergoes dehydration, and the thermogravimetric curve reflects the thermal changes of the composite membrane. The application of the composite membrane in high-temperature proton exchange membrane fuel cells holds significant importance.

In this study, the thermogravimetric analysis was conducted using the TGA-55 instrument from TA Instruments, USA. The measurements were performed under a nitrogen atmosphere, with a temperature range of 30–800°C and a heating rate of 10°C/min.

The mechanical properties of the composite membrane were analyzed using stress-strain curves to evaluate its elastic limit and ultimate strength. The impact of the modification scheme on the mechanical properties of the composite membrane was investigated.

The mechanical performance test was conducted using the C22-102 Universal Testing Machine from SanSi Corporation. The membrane was cut into strips measuring 0.5 cm × 4 cm and tested under room temperature conditions. The testing was performed with a tensile rate of 25 mm/min.

Before testing, the prepared high-temperature proton exchange membrane was cut into dimensions of 1 cm × 3 cm. Subsequently, the test membrane was immersed in a 1 mol/L hydrochloric acid solution for acid treatment. The proton conductivity measurements were conducted using a two-electrode method on the Interface 1000 Gamry electrochemical workstation. The testing frequency ranged from 0.1 Hz to 1 Hz. The proton conductivity testing was performed in the vertical direction of the membrane material, as described in the following equation:

$$\sigma = \frac{L}{R \cdot A}. \quad (4)$$

In the equation,  $\sigma$  represents the proton conductivity of the membrane,  $L$  and  $R$  are the resistances associated with the thickness of the membrane, and  $A$  represents the area of the electrode.

### 3. Results and Discussion

**3.1. Doping Level of  $\text{SiO}_2$ .** The doping ratio of  $\text{SiO}_2$  provides a visual indication of the effectiveness of Nafion membrane modification. According to Table 1, it can be observed that the composite membrane manufactured at 30°C exhibits a relatively lower  $\text{SiO}_2$  doping ratio compared to the one manufactured under low-temperature conditions. This suggests that the doping efficiency of  $\text{SiO}_2$  is higher under low-temperature conditions. Furthermore, at the same temperature, the composite membrane with a doping time of 5 minutes shows a higher doping level, indicating that the  $\text{SiO}_2$  within the membrane has not reached a saturation state yet.

**3.2. SEM and EDS Analysis.** To investigate the distribution of  $\text{SiO}_2$  particles in the composite membrane, both the surface and cross-section of the Nafion/ $\text{SiO}_2$  series membranes and Nafion membrane were characterized using SEM. The surface characterization results are shown in Figures 1 and 2. Figures 1(d) and 2(d) depict the SEM images of the surface of the Nafion membrane without  $\text{SiO}_2$  introduction. The Nafion membrane appears highly uniform and dense, without any noticeable defects. With the introduction of  $\text{SiO}_2$ , as a dispersed phase, the  $\text{SiO}_2$  particles are uniformly distributed within the Nafion matrix. Figures 1(a) and 2(a) show the SEM images of the surface of the composite membrane manufactured at 30°C. It can be observed from the SEM images that there are noticeable pores on the membrane surface, indicating the nonuniform dispersion of  $\text{SiO}_2$  particles within the Nafion membrane. Figures 1(b) and 1(c) and 2(b) and 2(c) demonstrate that under low-temperature conditions and a doping time of 3 minutes, the  $\text{SiO}_2$  particles are uniformly distributed as a dispersed phase within the Nafion matrix, where the Nafion matrix fully encapsulates the  $\text{SiO}_2$  particles. With increasing doping time, the  $\text{SiO}_2$  particles gradually form a continuous phase within the Nafion matrix.

The cross-sectional characterization results are shown in Figure 3. Figures 3(a) and 3(b) correspond to composite membranes fabricated at 30°C and with a doping time of 3 minutes under low-temperature conditions, respectively. From the SEM images, it can be observed that both types of composite membranes exhibit rough surfaces and cracks. Figure 3(c) represents a composite membrane produced with a doping time of 5 minutes under low-temperature conditions, and its cross-section appears to be smooth and flat. The possibility of uneven  $\text{SiO}_2$  distribution or even aggregation is suggested by Figures 4(a) and 4(b). This speculation is confirmed by the results of Si element energy-dispersive X-ray spectroscopy (EDS) analysis. Since the Si element is only present in silica, the distribution of the Si



TABLE 1: Doping ratio of SiO<sub>2</sub> in high-temperature proton exchange membranes.

Sample	Nafion/SiO <sub>2</sub> 30°C	Nafion/SiO <sub>2</sub> 3°C-3	Nafion/SiO <sub>2</sub> 3°C-5
Si uptake (%)	14.94%	15.57%	19.26%

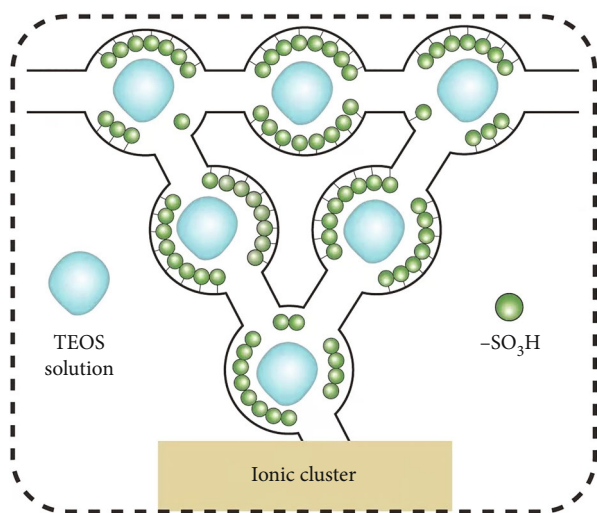


FIGURE 1: TEOS schematic diagram.

element represents the distribution of SiO<sub>2</sub> nanoparticles. The test results indicate that SiO<sub>2</sub> is uniformly distributed throughout the entire Nafion/SiO<sub>2</sub>3°C-5 membrane.

**3.3. FT-IR Analysis.** The prepared composite membranes and Nafion membranes were subjected to infrared spectroscopy testing, as shown in Figure 5. The infrared spectra of Nafion/SiO<sub>2</sub> composite membranes prepared with different processing schemes were essentially consistent. A comparison between the infrared spectra of Nafion/SiO<sub>2</sub> composite membranes and Nafion membranes revealed the appearance of new diffraction peaks in the composite membranes. Two new diffraction peaks were observed at 446 and 1081 cm<sup>-1</sup>, corresponding to the characteristic peaks of Si-O-Si and Si-OH, respectively. Furthermore, no significant diffraction peaks were observed in the infrared spectra of the composite membranes, indicating that the incorporation of silicon dioxide during the Nafion matrix did not result in excessive deposition or uneven distribution. Therefore, the characteristic peaks were not prominent.

The results demonstrate that Si nanoparticles have been successfully incorporated into the composite membranes without any other impurities. Compared to other composite membranes, the distribution of silicon dioxide within the Nafion/SiO<sub>2</sub>3°C-5 composite membrane is more uniform.

**3.4. XRD Analysis.** The prepared composite membrane and the Nafion membrane were subjected to XRD testing to obtain morphological information about the composite membrane, particularly information regarding its crystallinity. As shown in Figure 6, there are two broad diffraction peaks at 2θ~17° and 2θ~38 degrees. These two broad diffraction peaks originate from the convolution of Nafion's amorphous and crystalline scattering as well as the amorphous

stacking of Nafion chains. It is evident from the graph that after doping with SiO<sub>2</sub>, the peaks of the composite membrane are noticeably broader than those of Nafion. This is because SiO<sub>2</sub> is amorphous, indicating its amorphous characteristics. The Nafion/SiO<sub>2</sub> composite membrane, prepared under low-temperature conditions, has altered the microstructure and crystallinity of the Nafion membrane. The broadening of the peaks in the composite membrane suggests that the structure of the composite membrane remains amorphous.

Microscopic characterization experiments were conducted on the Nafion/SiO<sub>2</sub> composite membrane. The experimental results demonstrate that silicon (Si) nanoparticles have been successfully incorporated into the composite membrane without the presence of other impurities. In comparison to other composite membranes, the distribution of silicon dioxide (SiO<sub>2</sub>) within the Nafion/SiO<sub>2</sub>3°C-5 composite membrane is more uniform.

**3.4.1. Water Uptake and Swelling Ratio.** The water absorption and volume swelling of the Nafion/SiO<sub>2</sub> composite membrane were measured, and these two properties are closely related parameters reflecting the interaction of proton exchange membranes in water. Water absorption refers to the membrane's ability to absorb water in aqueous environments. In fuel cells, proton conduction primarily depends on water molecules, making the water-retaining capacity of proton exchange membranes crucial. After water absorption, proton exchange membranes experience a certain degree of expansion in overall volume. Excessive swelling can reduce the mechanical strength of the proton exchange membrane, affecting the operational stability and lifespan of proton exchange membrane fuel cells.

The calculated results are presented in Table 2. Data comparison reveals that the water absorption of the SiO<sub>2</sub>-doped composite membrane is higher than that of the pure Nafion membrane. This is attributed to the excellent porous structure and surface area of silica (SiO<sub>2</sub>), along with its strong adsorption capacity, which enhances the water-retaining ability of the proton exchange membrane. With changes in doping temperature and time, the water absorption of the Nafion/SiO<sub>2</sub>3°C-5 composite membrane reached 29.23%. The volume swelling of the Nafion/SiO<sub>2</sub>30°C composite membrane is 4.89% higher than that of the pure Nafion membrane, indicating poorer size stability of the composite membrane manufactured at 30°C. The volume swelling rates of the Nafion/SiO<sub>2</sub>3°C-3 and Nafion/SiO<sub>2</sub>3°C-5 composite membranes are relatively low, indicating a more uniform doping of silica in the matrix at low temperatures, thereby improving the size stability of the composite membrane.

**3.4.2. Thermal Stability.** The thermodynamic performance of high-temperature proton exchange membranes is crucial, and this performance indicator effectively reveals the

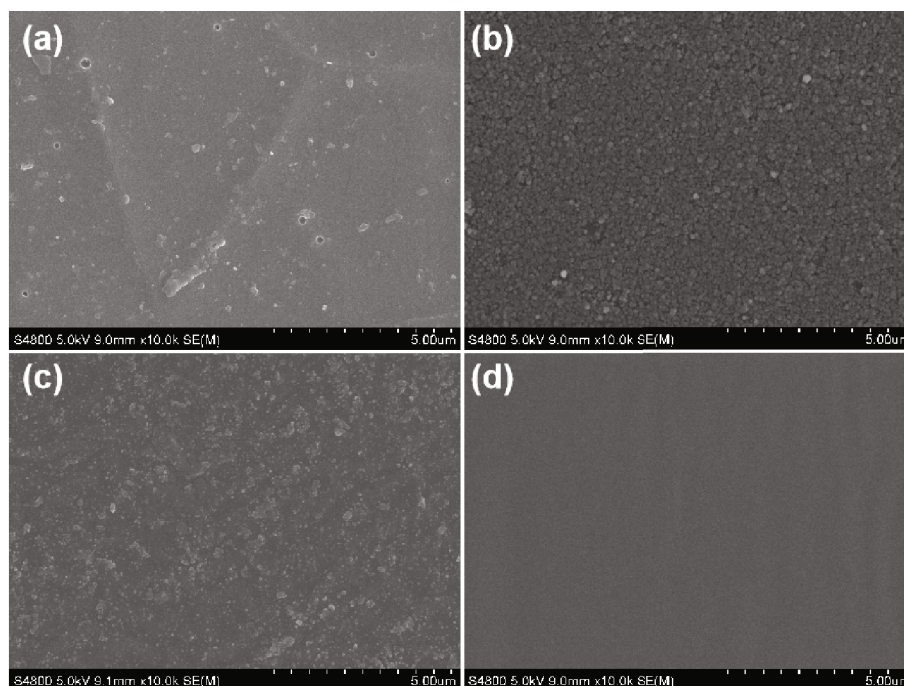


FIGURE 2: SEM images (5  $\mu\text{m}$ ) of the proton exchange membrane surface: Nafion/SiO<sub>2</sub>30°C (a), Nafion/SiO<sub>2</sub>3°C-3 (b), Nafion/SiO<sub>2</sub>3°C-5 (c), and Nafion (d).

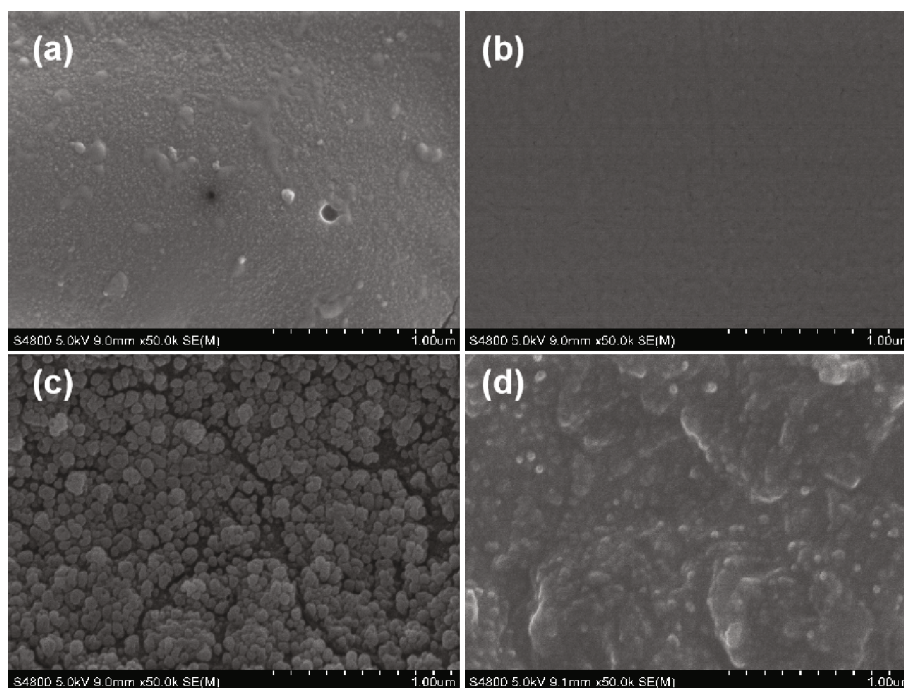


FIGURE 3: SEM images (1  $\mu\text{m}$ ) of the proton exchange membrane surface: Nafion/SiO<sub>2</sub>30°C (a), Nafion/SiO<sub>2</sub>3°C-3 (b), Nafion/SiO<sub>2</sub>3°C-5 (c), and Nafion (d).

stability of the composite membrane prepared in high-temperature environments. This helps prevent irreversible degradation or changes in the composite membrane at elevated temperatures. As shown in the thermal gravimetric analysis (TGA) curve in Figure 7, the decay rate of the Nafion/SiO<sub>2</sub>30°C composite membrane is significantly

higher than that of the pure Nafion membrane. Combined with the conclusions drawn from the earlier swelling rate tests, it indicates that the internal structure of the Nafion/SiO<sub>2</sub>30°C composite membrane has been compromised during the doping process. In contrast, the Nafion/SiO<sub>2</sub>3°C-3 and Nafion/SiO<sub>2</sub>3°C-5 composite membranes exhibit a



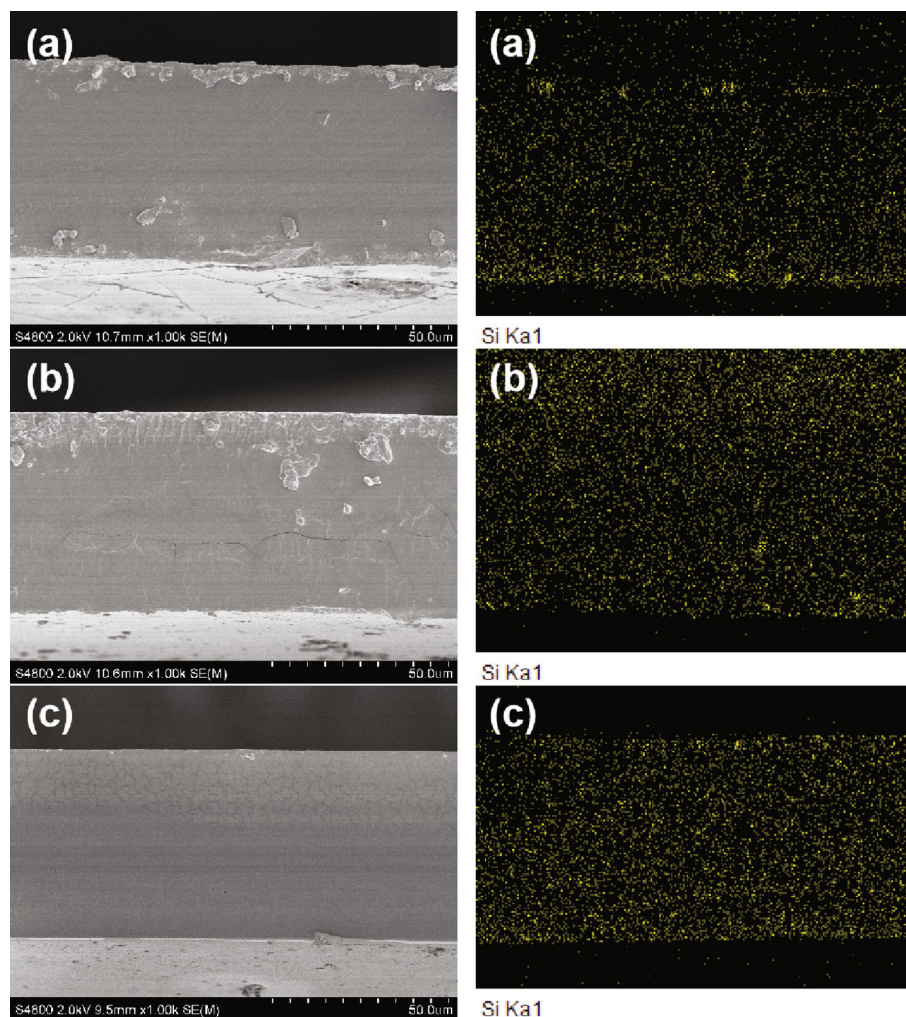


FIGURE 4: SEM images of cross-sections of Nafion composite membranes and EDS mapping of Si element: Nafion/SiO<sub>2</sub>30°C (a), Nafion/SiO<sub>2</sub>3°C-3 (b), and Nafion/SiO<sub>2</sub>3°C-5 (c).

substantial decline at around 440°C, whereas the Nafion membrane starts to experience a significant decline at 470°C. Despite the relatively intact microstructure of the composite membrane doped at low temperatures, it still has a slight impact on the thermal weight loss performance of the membrane. Compared to the 30°C composite membrane, the Nafion/SiO<sub>2</sub>3°C-3 and Nafion/SiO<sub>2</sub>3°C-5 composite membranes demonstrate better performance in high-temperature environments.

**3.4.3. Mechanical Stability.** Proton exchange membranes in fuel cells are subjected to various forms of mechanical stress, such as vibration, pressure, and deformation. Additionally, the working environment of proton exchange membranes may experience fluctuations in temperature and humidity, potentially impacting the volume of the proton exchange membrane. If the mechanical strength of the membrane is insufficient, it can lead to damage during operation. Therefore, the mechanical strength of proton exchange membranes is an important testing parameter. The mechanical performance test of the composite membrane is shown in

Figure 8. Silica particles themselves have high hardness and rigidity. When silica particles are doped into the matrix, they can affect the mechanical strength of the membrane to some extent. From Figure 8, it is evident that the maximum tensile stress of the Nafion/SiO<sub>2</sub>30°C composite membrane is significantly lower compared to the pure Nafion membrane. Combining the previous swelling rate test results, excessive expansion of the membrane has a significant impact on its mechanical strength.

In contrast, the mechanical strength of the Nafion/SiO<sub>2</sub>3°C-3 and Nafion/SiO<sub>2</sub>3°C-5 composite membranes prepared at low temperatures is not affected and is slightly higher than that of the Nafion membrane. The maximum tensile strength of the Nafion/SiO<sub>2</sub>3°C-5 composite membrane reaches 274 MPa, and the fracture elongation rate also reaches 270%. This indicates that the in situ sol-gel reaction conducted at low temperatures effectively controls the hydrolysis rate of tetraethyl orthosilicate (TEOS). The hydrolysis product, ethanol, can be promptly released from the composite membrane, reducing the risk of excessive membrane expansion.

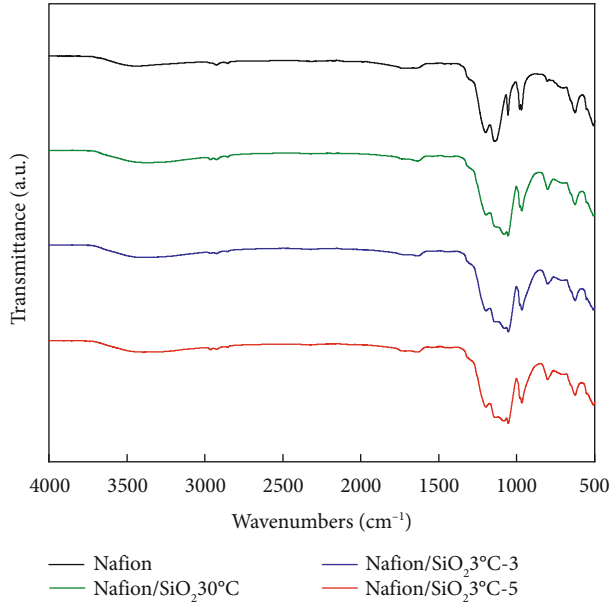


FIGURE 5: FT-IR spectra of Nafion membrane and composite membranes.

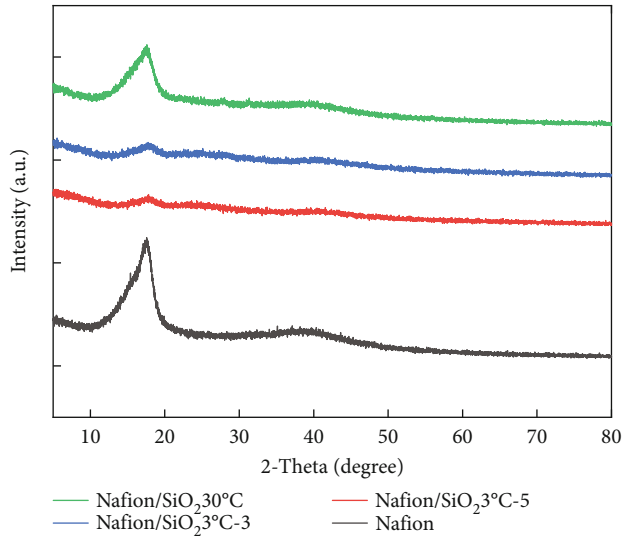


FIGURE 6: XRD spectra of Nafion membrane and composite membrane.

TABLE 2: Water uptake and volume swelling ratio of Nafion membrane and Nafion/SiO<sub>2</sub> composite membranes.

Sample	Water uptake	Volume swelling
Nafion	18.62%	26.37%
Nafion/SiO <sub>2</sub> 30°C	28.21%	31.26%
Nafion/SiO <sub>2</sub> 3°C-3	24.79%	25.52%
Nafion/SiO <sub>2</sub> 3°C-5	29.23%	24.45%

**3.4.4. Proton Conductivity.** Proton conductivity provides a direct indication of the proton-conducting capability of proton exchange membranes and is a crucial metric for asses-

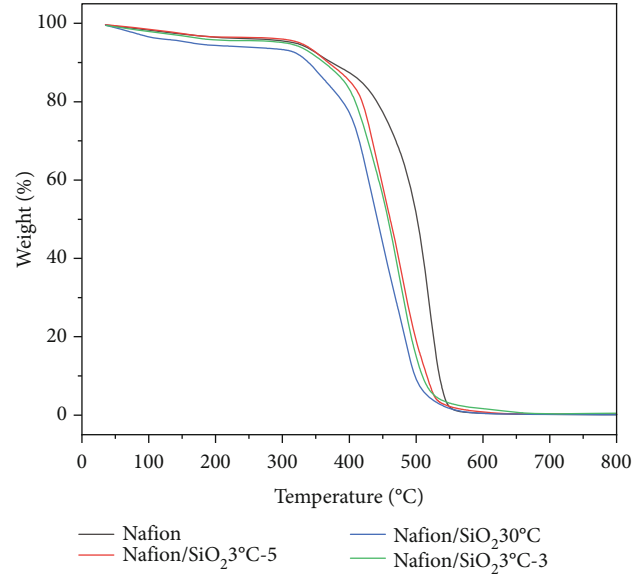


FIGURE 7: Thermal weight loss curves of Nafion and composite membranes.

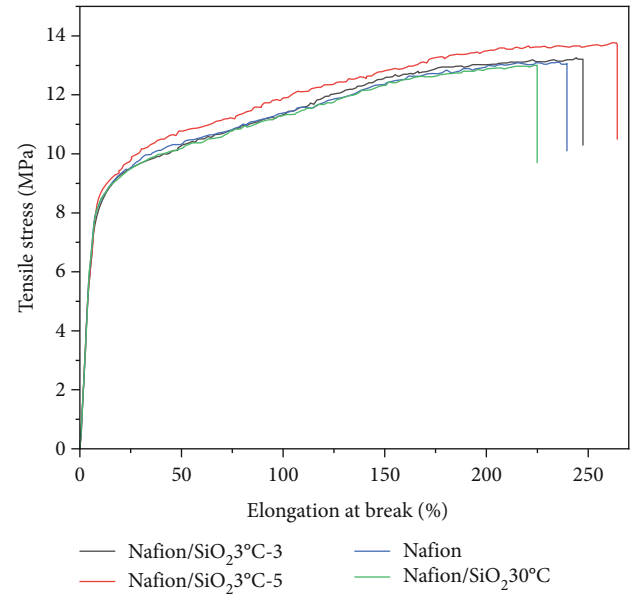


FIGURE 8: Stress-strain curves of Nafion and composite membranes.

sing their performance. A higher proton conductivity in the membrane signifies efficient proton conduction. In proton exchange membrane fuel cells, outstanding proton conductivity contributes to reducing resistance, enhancing energy conversion efficiency, and thereby improving the overall performance of fuel cells. Moreover, the improvement in proton conductivity also aids in reducing the transfer resistance of protons at the membrane electrode interface, lowering fuel cell polarization losses, and ensuring that the fuel cell maintains a higher range of current and power density.



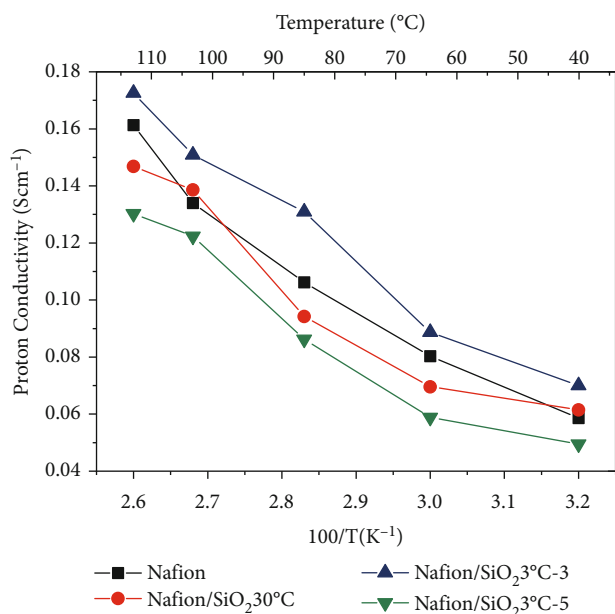


FIGURE 9: The graph depicting the variation of proton conductivity with temperature for Nafion and composite membranes.

Figure 9 illustrates the proton conductivity of Nafion membrane and composite membranes doped with  $\text{SiO}_2$  at different temperatures. As shown in the graph, the proton conductivity of both Nafion membrane and composite membranes gradually increases with temperature. For instance, at 40°C, the conductivity of the Nafion membrane is 0.057 S/cm, and it rises to 0.163 S/cm at 110°C. With the addition of  $\text{SiO}_2$  and variations in doping conditions, the proton conductivity of the membrane undergoes changes. It is evident from the graph that the Nafion/ $\text{SiO}_2$  3°C-3 composite membrane prepared at low temperatures achieves a proton conductivity of 0.172 S/cm at 110°C, surpassing that of the Nafion membrane at the same temperature and also exceeding the proton conductivity of the Nafion/ $\text{SiO}_2$  3°C-5 composite membrane. This indicates that the doping of silicon dioxide enhances the water retention capacity of the proton exchange membrane under low-temperature conditions. However, a 5-minute doping time leads to internal aggregation in the membrane, hindering the provision of additional channels for proton transfer.

#### 4. Conclusions

In summary, this study utilizes silicon dioxide as an inorganic filler and selects tetraethyl orthosilicate (TEOS) as the precursor. Based on an in situ sol-gel reaction and varying reaction conditions, three silicon dioxide-modified composite membranes, namely, Nafion/ $\text{SiO}_2$  30°C, Nafion/ $\text{SiO}_2$  3°C-3, and Nafion/ $\text{SiO}_2$  3°C-5, are prepared. The microstructures and proton transport properties of these three membranes are investigated. Tetraethyl orthosilicate, an excellent silicon dioxide precursor, facilitates the incorporation of silicon dioxide into the Nafion matrix. However, the hydrolysis reaction of this solution produces a significant amount of ethanol. Residual ethanol in the Nafion matrix

can lead to membrane swelling, thereby compromising its performance. In comparison to traditional in situ sol-gel reactions, the preparation in this study reduces the reaction temperature from 30°C to 3°C. Lowering the temperature allows better control of the reaction of tetraethyl orthosilicate (TEOS) and promotes the expulsion of ethanol. SEM results clearly show that the composite membrane prepared at low temperatures exhibits a complete structure, with silicon dioxide uniformly distributed in the Nafion matrix and no pore formation. Elemental distribution testing for silicon (Si) further supports this observation, confirming the even distribution of Si elements within the membrane. Additional FT-IR and XRD tests on the composite membrane demonstrate the uniform incorporation of silicon dioxide into the Nafion212 membrane. Calculations of water absorption and swelling indicate that the composite membrane prepared at low temperatures does not experience excessive swelling in high-humidity environments and can efficiently conduct protons in low-humidity conditions. This indirectly confirms the formation of a stable framework structure with silicon dioxide supporting clusters alongside the Nafion main chain. Thermal weight loss testing results confirm the formation of a stable framework network of silicon dioxide in the matrix. Compared to other methods for preparing silicon dioxide-modified Nafion composite membranes, the in situ sol-gel reaction offers higher efficiency, although the uncontrollable hydrolysis reaction can affect the mechanical strength of the composite membrane. Stress-strain curve results show that the composite membrane prepared at low temperatures maintains higher water absorption, while, compared to the Nafion membrane, it exhibits a stable improvement in mechanical strength. This suggests that the composite membrane prepared at low temperatures still possesses a stable structure. In high-temperature fuel cell operation, the rapid loss of water molecules leads to a sharp decline in the proton conductivity of Nafion membranes, significantly impacting the efficiency of fuel cells. Silicon dioxide, as a hydrophilic inorganic material, if stably incorporated into the cluster structure within the Nafion matrix, can enable the prepared composite membrane to adapt to high-temperature, low-humidity operating environments. The proton conductivity of Nafion/ $\text{SiO}_2$  3°C-3 at 110°C reaches 0.172 S/cm, exhibiting a stable improvement compared to the Nafion membrane. The composite membranes prepared by reducing the reaction temperature provide a solution for the application of Nafion/ $\text{SiO}_2$  composite membranes in high-temperature proton exchange membrane fuel cells.

#### Data Availability

The authors confirm that the data supporting the findings of this study are available within the article.

#### Conflicts of Interest

The authors state no conflict of interest.

## Acknowledgments

This research was supported by the Guangxuan Program Funding Project of Shenyang Ligong University and Liaoning Provincial Department of Education (LJKMZ20220601), and the authors would like to express their appreciation to them.

## References

- [1] A. Kusoglu and A. Z. Weber, "New insights into perfluorinated sulfonic-acid ionomers," *Chemical Reviews*, vol. 117, no. 3, pp. 987–1104, 2017.
- [2] H. Wang, J. Zhang, X. Ning, M. Tian, Y. Long, and S. Ramakrishna, "Recent advances in designing and tailoring nanofiber composite electrolyte membranes for high-performance proton exchange membrane fuel cells," *International Journal of Hydrogen Energy*, vol. 46, no. 49, pp. 25225–25251, 2021.
- [3] M. M. Nasef, "Radiation-grafted membranes for polymer electrolyte fuel cells: current trends and future directions," *Chemical Reviews*, vol. 114, no. 24, pp. 12278–12329, 2014.
- [4] J. Zhang, Y. Tang, C. Song, X. Cheng, J. Zhang, and H. Wang, "PEM fuel cells operated at 0% relative humidity in the temperature range of 23–120 °C," *Electrochimica Acta*, vol. 52, no. 15, pp. 5095–5101, 2007.
- [5] S. Authayanun, M. Mamlouk, K. Scott, and A. Arpornwichanop, "Comparison of high-temperature and low-temperature polymer electrolyte membrane fuel cell systems with glycerol reforming process for stationary applications," *Applied Energy*, vol. 109, pp. 192–201, 2013.
- [6] S. J. Osborn, M. K. Hassan, G. M. Divoux, D. W. Rhoades, K. A. Mauritz, and R. B. Moore, "Glass transition temperature of perfluorosulfonic acid ionomers," *Macromolecules*, vol. 40, no. 10, pp. 3886–3890, 2007.
- [7] H. Y. Jung and J. W. Kim, "Role of the glass transition temperature of Nafion 117 membrane in the preparation of the membrane electrode assembly in a direct methanol fuel cell (DMFC)," *International Journal of Hydrogen Energy*, vol. 37, no. 17, pp. 12580–12585, 2012.
- [8] V. Di Noto, R. Gliubizzi, E. Negro, and G. Pace, "Effect of SiO<sub>2</sub> on relaxation phenomena and mechanism of ion conductivity of [Nafion/(SiO<sub>2</sub>)<sub>x</sub>] composite membranes," *The Journal of Physical Chemistry B*, vol. 110, no. 49, pp. 24972–24986, 2006.
- [9] C. C. Ke, X. J. Li, S. G. Qu, Z. G. Shao, and B. L. Yi, "Preparation and properties of Nafion/SiO<sub>2</sub> composite membrane derived via in situ sol–gel reaction: size controlling and size effects of SiO<sub>2</sub> nano-particles," *Polymers for Advanced Technologies*, vol. 23, no. 1, pp. 92–98, 2012.
- [10] Y. F. Lin, C. Y. Yen, C. C. M. Ma et al., "High proton-conducting Nafion®/–SO<sub>3</sub>H functionalized mesoporous silica composite membranes," *Journal of Power Sources*, vol. 171, no. 2, pp. 388–395, 2007.
- [11] D. Zhao, B. L. Yi, H. M. Zhang, and H. M. Yu, "MnO<sub>2</sub>/SiO<sub>2</sub>–SO<sub>3</sub>H nanocomposite as hydrogen peroxide scavenger for durability improvement in proton exchange membranes," *Journal of Membrane Science*, vol. 346, no. 1, pp. 143–151, 2010.
- [12] M. A. Dresch, R. A. Isidoro, M. Linardi, J. F. Q. Rey, F. C. Fonseca, and E. I. Santiago, "Influence of sol–gel media on the properties of Nafion–SiO<sub>2</sub> hybrid electrolytes for high performance proton exchange membrane fuel cells operating at high temperature and low humidity," *Electrochimica Acta*, vol. 94, pp. 353–359, 2013.
- [13] J. Choi, J. H. Yeon, S. H. Yook et al., "Multifunctional Nafion/CeO<sub>2</sub> dendritic structures for enhanced durability and performance of polymer electrolyte membrane fuel cells," *ACS Applied Materials & Interfaces*, vol. 13, no. 1, pp. 806–815, 2021.
- [14] H. Wang, X. Li, X. Zhuang et al., "Modification of Nafion membrane with biofunctional SiO<sub>2</sub> nanofiber for proton exchange membrane fuel cells," *Journal of Power Sources*, vol. 340, pp. 201–209, 2012.